Friction https://mc03.manuscriptcentral.com/friction
https://doi.org/10.26599/FRICT.2026.9441234

Research Article

Supramolecular composite gel lubricants with polymer brush-grafted MOFs additives for enhanced friction and wear reduction

Yong Qian[1,#], Haowen Luo[1,#], Lejie Tian[1], Haohui Yang[1], Bin Li[3], Long Wang[1], Dongsheng Li[2]✉, Feng Zhou[3], Jianxi Liu[1]✉

#Yong Qian and Haowen Luo contributed equally to this work

[1]State Key Laboratory of Solidification Processing, Center of Advanced Lubrication and Seal Materials, School of Materials Science and Engineering, Northwestern Polytechnical University, Xi'an 710072, China

[2]Shaanxi Engineering Research Center of Special Sealing Technology, Xi'an Aerospace Propulsion Institute, Xi'an 710100, China

[3]State Key Laboratory of Solid Lubrication, Lanzhou Institute of Chemical Physics, Chinese Academy of Sciences, Lanzhou 730000, China

✉ Corresponding authors. E-mail: Dongsheng Li, lidsh1013@163.com; Jianxi Liu, jianxiliu@nwpu.edu.cn

Received: September 29, 2025; Revised: January 28, 2026; Accepted: February 20, 2026

Abstract: Supramolecular gel holds great potential in engineering applications as lubricant. However, pure organic network of the gel limits their rheological and lubrication performance. Here, we report a nanoporous materials-functionalized supramolecular composite gel lubricant by incorporating polymer brush-grafted metal-organic frameworks (MOFs) nanoparticles (NPs) as nano additive. The composite gel was produced by encapsulating poly(lauryl methacrylate) (PLMA) polymer brushes functionalized UiO-67 (UiO-67@PLMA) NPs in 500 SN base oil of a 3D network formed by 12-hydroxystearic acid (12-HSA) through hydrogen bonding and van der Waals (vdW) interactions. The addition of UiO-67@PLMA NPs largely improved the thermal and rheological properties of the 12-HAS/500 SN gel, and the storage modulus and loss modulus increasing significantly. Tribological tests showed that incorporating 0.40 wt.% UiO-67@PLMA NPs into the composite gel reduced the coefficient of friction and wear volume by 45.68% and 86.85%, respectively. Furthermore, the UiO-67@PLMA gel demonstrated remarkable tribological performance under challenging conditions, such as 400 N, 65 Hz, and 160 °C. The outstanding lubrication performance of the supramolecular composite gel arises from shear-triggered release of base oil and nanoadditves, acting as nano ball-bearings and promoting protective film formation.

Keywords: Supramolecular gel, MOFs, PLMA, Friction reduction, Anti-wear

1 Introduction

Supramolecular gels, composed of a gelling agent and a base oil, represent a class of materials positioned between solids and liquids [1, 2]. Through non-covalent interactions like hydrogen bonding, hydrophilic-hydrophobic interactions, and host-guest interactions, the gel agent self-assembles into a three-dimensional (3D) network that immobilized the base oil [3, 4]. These weak interactions can be disrupted by thermal stress or mechanical shear, enabling reversible conversion between gel and sol states [5]. In particular, supramolecular gels co-assemble with aromatic peptides and polyethylene

glycol undergo reversible gel-sol transitions under temperature changes [6]. Supramolecular gels are self-assembled under shear force conditions. When shearing force is applied through a vortex oscillator, the resulting mixture changes from sol to gel. Also, the gel could gradually relax back to a sol [7].

Current research on supramolecular gels primarily focuses on synthesizing new gel agents to fabricate pure supramolecular gel lubricants [8]. Minakuchi et al. [9] developed low molecular weight gel factors with polyhydroxyl groups, and introduced amino acids to increase the structural diversity, achieving efficient capture of a variety of solvents and ionic liquids. Yu et al. [10] synthesized a self-assembled amphiphilic gel via electrostatic interactions. They explored the thermorheological properties and compared with lithium-based and MoS_2-functionalized lithium-based greases, proofing the excellent lubrication properties of the amphiphilic molecular gel. Bai et al [11] demonstrated that using the gel matrix to stabilize additives is powerful on Perfluoropolyether oils, and developed a supramolecular gel entrapping MoS_2 nanoparticles (NPs) within its 3D network to prevent aggregation and settling. This gel@MoS_2 composite not only achieved exceptional dispersion stability but also significantly enhanced the mechanical strength, extreme pressure performance, and anti-wear properties of the lubricant under high load, showcasing a direct link between additive integration and superior functional performance. Hence, these studies have shown that incorporating additives can further enhanced the tribological and rheological properties of gels, but the additional functionalities are impaired [12-14].

Metal-organic frameworks (MOFs) are 3D nanoporous materials composed of metal ions clusters coordinated to organic ligands [15-17]. Due to their tunable composition, large specific surface area, and excellent nanomechanical properties, MOFs have emerged as promising lubricant additives [18, 19]. For instance, small-sized zeolite imidazoline framework-8 (ZIF-8) NPs have been shown to enhance lubricity [20], while ZIF-71 particles added to liquid paraffin improved load-carrying and anti-wear performance [21]. In addition, the MOF surface has abundant chemically active sites, making it customizable for precise functionalization to ultimately improve the compatibility with base

oils [22, 23]. Oil-soluble dialkyldithiophosphate (DDP) molecules and poly(lauryl methacrylate) (PLMA) brushes modified UiO-67 NPs could significantly improve friction reduction and anti-wear properties [24-26]. As oil lubricating additives, however, there are still challenges for nanomaterials that eventually lead to aggregation due to gravity and intermolecular forces. Supramolecular gels are expected to provide more effective and longer-lasting lubrication in critical application and prevent environmental contamination such as oil creep.

In this work, we report a thermally reversible MOFs-based supramolecular composite gel lubricant exhibiting highly efficient friction reduction and anti-wear performance. To enhance the dispersion stability of UiO-67 NPs, PLMA polymer brushes were grafted onto their surface via surface-initiated atom transfer radical polymerization (SI-ATRP). The resulting UiO-67@PLMA NPs were encapsulated in a 3D network formed by 12-hydroxystearic acid (12-HSA) and 500 SN base oil through hydrogen bonding and van der Waals (vdW) interactions, and the three-dimensional network with nanoporous MOFs exhibits a dispersion stability of more than 50 days. Tribological tests revealed that the incorporation of UiO-67@PLMA significantly reduced the coefficient of friction (COF) and wear volume of the 500 SN gel. The UiO-67@PLMA composite gel owns excellent load-carrying capacity and durability, maintaining stable performance even under high-frequency (65 Hz) and high-temperature (160 °C) conditions. The nanoporous materials functionalized supramolecular composite gel promote a new lubricant system for friction and wear reduction under harsh conditions.

2 Experimental

2.1. Materials and Chemicals

Zirconyl chloride octahydrate ($ZrOCl_2 \cdot 8H_2O$, 99%), biphenyl-4,4′-dicarboxylic acid (H_2BPDC, 98%), and lauryl methacrylate (LMA, 97%) were purchased from Energy Chemical Co. Ltd. Acetic acid was purchased from Sinopharm Chemical Co. Ltd. 2-Hydroxyethyl methacrylate (HEMA, 98%), trifluoroacetic acid (TFA, 99%), CuBr (98%), N, N, N’, N’, N’’-pentamethyldiethylenetriamine (PMDETA, 99%), ethyl 2-bromoisobutyrate (BiBB, 98%), sodium chloride (NaCl, 99.5%), sodium

carbonate (Na_2CO_3, 99.5%), 2-methyl propionitrile (AIBN, 98%), anhydrous magnesium sulfate ($MgSO_4$, 99%), and triethylamine were purchased from Aldrich Co. Ltd. tert-Butyl methacrylate (tBuMA, 99%) was obtained from Energy Chemical Co. Ltd. N, N'-dimethylformamide (DMF), methanol, dichloromethane (DCM), toluene, and 12-HSA were purchased from Shannxi Dexiang Chemical Co. Ltd.

2.2. Synthesis of UiO-67 nanoparticles

UiO-67 ($Zr_6O_4(OH)_4(C_{14}H_8O_4)_6$) NPs were synthesized following a previously reported solvothermal method, with particle size modulation by acetic acid [27]. Specifically, 1.08 g of $ZrOCl_2 \cdot 8H_2O$ was dissolved in 360 mL of DMF to obtain a clear solution under stirring. Separately, 2.4 g of H_2BPDC was dissolved in 120 mL of DMF and was sociated for 30 minutes to form a homogeneous white suspension. The metal salt solution and the organic linker suspension were mixed in a three-necked flask. Then, acetic acid (0.5 M) was added, followed by sonication for 5 minutes. The mixture was then heated at 90 °C for 20 hours. The resulting UiO-67 NPs were divided into four portions and purified by centrifugation (13,000 rpm, 10 minutes) using DMF (3 times) and methanol (3 times), subsequently.

2.3. Synthesis of P(MAA-co-HEMBr) Macroinitiator

Synthesis of 2-(2-Bromoisobutyryloxy)ethyl methacrylate (HEMBr): HEMBr was synthesised according to previously reported methods [28]. Briefly, 21.4 mL of HEMA and 12.0 mL of triethylamine were added into a 250 mL three-neck flask, followed by adding 70 mL of DCM under an ice bath at 0 °C. After degassing with argon, 19.76 mL of BiBB dissolved in 23.1 mL of DCM was added dropwise in the cooled DCM solution. The reaction proceeded at 0 °C for 4 hours. The resulting mixture was filtered and washed with DCM. The organic phase was successively washed 3 times with saturated Na_2CO_3 and NaCl solutions. Anhydrous $MgSO_4$ was added to remove residual water, and the solvent was removed using a rotary evaporator, yielding a pale-yellow liquid.

Synthesis of P(tBuMA-co-HEMBr): 3.0 g of HEMABr, 169.4 mg of tBuMA, and 15 mg of AIBN were dissolved in 3 mL of DMF. After argon degassing, the solution was heated from 25 to 70 °C and maintained for 1 hour. The resulting polymer was precipitated several times in methanol and dried under vacuum.

Synthesis of P(MAA-co-HEMBr): The P(tBuMA-co-HEMBr) polymer was treated with TFA for 2 hours to remove t-butyl groups. The resulting macroinitiator, P(MAA-co-HEMBr), was purified by repeated precipitation in methanol and dried under vacuum overnight.

2.4. Synthesis of UiO-67@PLMA NPs

UiO-67@PLMA NPs were prepared by a two-step method as reported in our previous paper [26]. Initially, 50 mg of UiO-67 and 50 mg of the macroinitiator were dispersed in 50 mL of DCM. After stirring for 18 hours, the UiO-67@macronitiator was collected by centrifugation and washed with DCM and toluene. Subsequently, UiO-67@macronitiator, 6 g of LMA, 60 μL of PMDETA, and 6 mL of DMF were added to an ampule. After deoxygenation with argon, 30 mg of CuBr was introduced to active reaction. After polymerization for 1 hour, the UiO-67@PLMA NPs were synthesized, which were purified by washing with DMF (2 times) and DCM (3 times) to remove the catalyst and excess monomer.

2.5. Preparation of Supramolecular Composite Gels

To prepare the supramolecular composite gel, 0.5 wt.% of 12-HSA was added to 500 SN base oil in a sample vial. The mixture was heated at 80 °C until the 12-HSA was completely dissolved and then cooled to room temperature to form a composite gel. For composite gels containing UiO-67 NPs or UiO-67@PLMA NPs additives, ultrasonic dispersion of the additives in the base oil was performed before adding 12-HSA. Pure PAO10 gels and PAO10 gels containing UiO-67@PLMA NPs were similarly prepared by replacing the 500 SN oil with PAO10.

2.6. Characterizations

The morphologies of UiO-67 and UiO-67@PLMA NPs were observed using a Zeiss Gemini-500 field-emission scanning electron microscope (SEM) at an acceleration voltage of 5 kV and a FEI JEM-F200 field emission transmission electron microscope (TEM) operating at 200 KV. Fourier transform infrared spectra (FT IR, Bruker Tensor II) was used to analyze the chemical structures. Crystallinity was evaluated by X-ray diffraction (XRD, Bruker D8). Gel-sol transition temperatures ($T_{gel-sol}$) were determined using a differential scanning calorimeter (DSC, TA Q2000). Thermogravimetric analysis (TGA) was conducted using a Mettler Toledo instrument over 100−600 °C. The tribological properties were evaluated using an SRV-V tribometer and a GTK-18-0433 3D surface profiler.

3 Manuscript preparation

3.1 Preparation of UiO-67@PLMA supramolecular composite gel

Scheme 1 illustrates the preparation process of the UiO-67@PLMA supramolecular composite gel. The secondary building units of UiO-67, constructed from zirconium ions and oxygen atoms, expose numerous unsaturated coordinative sites for further functionalization.

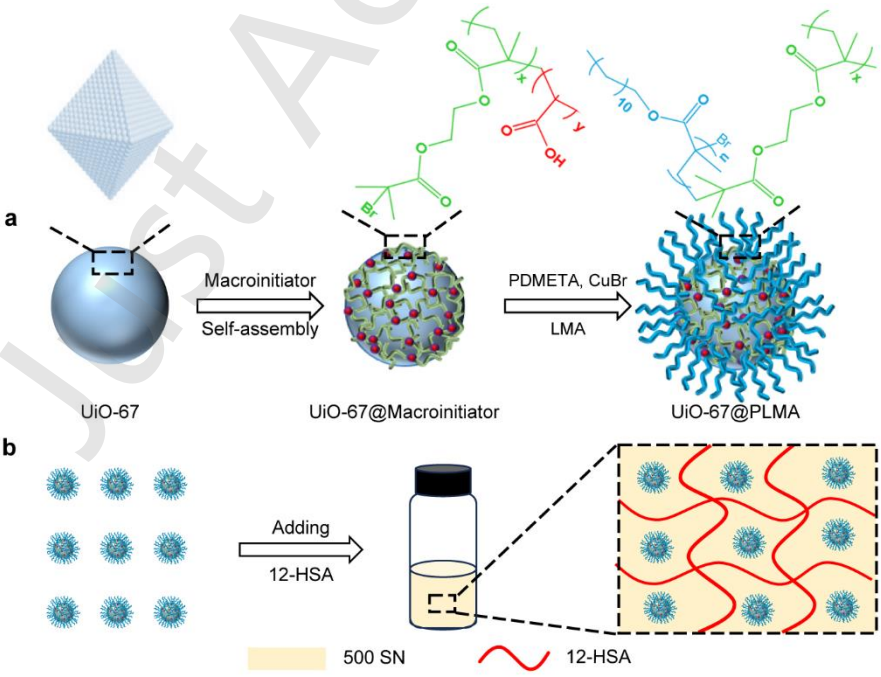

Scheme 1 Schematic illustration of the UiO-67@PLMA supramolecular composite gel preparation. (a) Synthesis of the UiO-67@PLMA NPs. (b) Formation of UiO-67@PLMA composite gel.

In this work, P(MAA-co-HEMBr) macroinitiators were assembled onto the surface of UiO-67 via coordination interactions between the carboxylic acid groups of the macroinitiator and the zirconium cluster sites (**Scheme 1a**). Subsequently, PLMA brushes were grown from the macroinitiator-modified UiO-67 surface through SI-ATRP, catalyzed by PMDETA and CuBr complexes [26]. In this way, UiO-67@PLMA NPs were successfully prepared. The preparation of the supramolecular composite gel is shown in **Scheme 1b**. 12-HSA molecules are able to form a 3D network via hydrogen bonding and vdW interactions by adding in 500 SN base oils (**Fig. S1**). The incorporation of UiO-67@PLMA NPs additives was effectively confined within the 3D network. Upon heating above the melting point, the long alkyl chains of 12-HSA exhibited good compatibility with the 500 SN base oils to show a liquid state (**Fig. S2**). Upon cooling, the base oil and additives were physically entrapped within the gel framework, resulting in the formation of the UiO-67@PLMA supramolecular composite gel.

3.2 Topographical and physicochemical properties of UiO-67@PLMA

The morphology of UiO-67 and UiO-67@PLMA NPs was characterized using SEM and TEM. As shown in **Figs. 1a-b**, the particle size of UiO-67 was approximately 83.7 ± 20 nm. Severe agglomeration was observed due to the high surface energy of UiO-67 NPs. After grafting PLMA brushes onto the UiO-67 surface, the composite NPs retained their original morphology and size, but the agglomeration was significantly reduced (**Fig. 1c**). Energy dispersive spectrometry (EDS) element mapping (**Fig. 1d**) revealed a uniform distribution of carbon (C) and zirconium (Zr) with a lower abundance of bromine (Br), confirming the successful grafting of PLMA onto UiO-67 NPs.

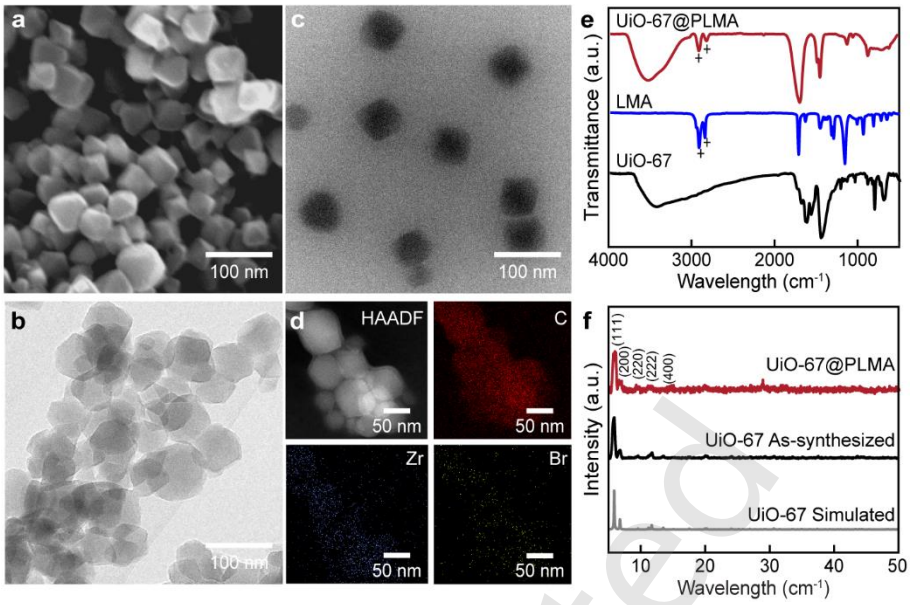

Fig. 1 Morphology and surface characterization of UiO-67 NPs before and after PLMA grafting. (a) SEM image of UiO-67 NPs. TEM images of (b) UiO-67 NPs and (c) UiO-67@PLMA NPs. (d) High-angle annular dark-field (HAADF) image of UiO-67@PLMA NPs and EDS mapping of C, Zr, and Br elements. (e) FTIR spectra. (f) XRD patterns.

Further confirmation of PLMA surface modification was provided by FTIR spectroscopy (**Fig. 1e**). Compared to pristine UiO-67, UiO-67@PLMA exhibited new absorption peaks corresponding to the symmetric and asymmetric stretching vibrations of C-H bonds at 2854 cm^{-1} and 2920 cm^{-1}, respectively, attributed to the alkane long chains of PLMA brushes [29]. XRD patterns (**Fig. 1f**) revealed characteristic peaks at 5.4°, 6.3°, 9.2°, 11.3° and 13.1°, corresponding to the (111), (200), (220), (222) and (400) crystallographic planes of UiO-67. After PLMA grafting, the diffraction peaks of UiO-67@PLMA remained consistent with those of pristine and simulated UiO-67, indicating that the crystallinity and phase purity of the UiO-67 framework were well preserved. Overall, these results confirm that UiO-67@PLMA NPs were successfully fabricated without altering their morphology, size, or crystalline structure.

3.3 Dispersibility of UiO-67@PLMA supramolecular composite gels

To evaluate the dispersibility of the different types of nanoadditives, the UiO-67 NPs with and without grafted with PLMA polymer brush, were dispersed as additives in 500 SN base oil and in 12-HAS/500

SN gel (500 SN gel). The samples were then left to stand for visual observation. In the base oil, the unmodified UiO-67 NPs exhibited a tendency to agglomerate and sediment over time due to their high surface energy and gravitational effects (**Fig. 2a).** Clear phase separation was observed after 3 days, with UiO-67 NPs visibly settled at the bottom of the container. In contrast, UiO-67@PLMA NPs maintained good dispersion under the same conditions (**Fig. 2b**), which can be attributed to the lipophilic nature of the PLMA polymer brushes and the associated reduction in interfacial energy between the MOF NPs and the oil. However, after 30 days, slight sedimentation of UiO-67@PLMA in 500 SN was noted, and by 50 days, clear delamination occurred, indicating limited long-term colloidal stability in the absence of structural reinforcement.

Upon introducing 12-HAS to the base oil, a supramolecular composite gel network was formed via hydrogen bonding and vdW interactions (**Fig. 2c**-**d**). Upon cooling, this 3D network effectively entrapped the additives, preventing their sedimentation and thereby enhancing their long-term stability. Due to their poor intrinsic dispersibility in base oil, UiO-67 NPs exhibited severe aggregation in the gel matrix, resulting in non-uniform color distribution (**Fig. 2c**). Conversely, the long alkyl chains of the PLMA brushes significantly could improve the dispersion of UiO-67@PLMA in the composite gel. As a result, the composite gels exhibited uniform coloration and a translucent appearance, which was maintained even after 50 days of storage (**Fig. 2d**). These results demonstrate that the formation of a 3D network by 12-HAS is effective in stabilizing the NPs additives dispersion, and the surface modification of UiO-67 with PLMA further enhances the dispersibility and long-term stability of the supramolecular composite gels.

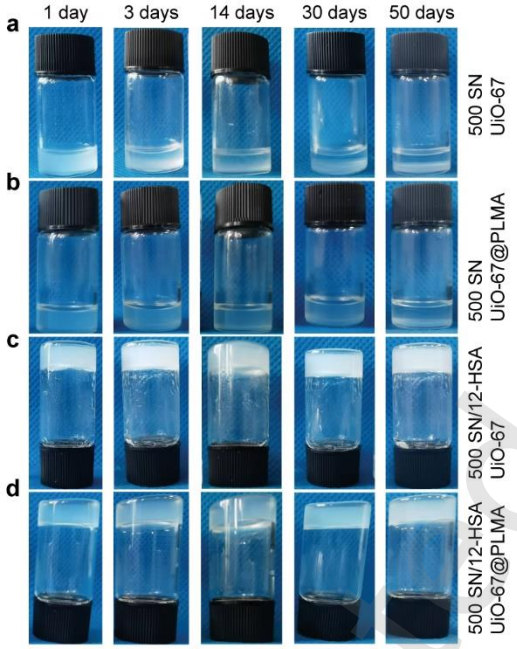

Fig. 2 Long-term dispersibility enhancement of UiO-67 NPs in 500 SN base oil and 12-HAS/500 SN composite gel before/after PLMA grafting. UiO-67 NPs dispersed in (a) 500 SN base oil and (c) 12-HAS/500 SN gel. UiO-67@PLMA NPs dispersed in (b) 500 SN and (d) 12-HAS/500 SN gel.

3.4 Thermorheological properties of supramolecular composite gels

The reversibility of supramolecular gels has been confirmed in various studies, which is an essential feature of supramolecular gels. The effect of heat causes 12-HSA to melt in the base oil, and then during the cooling process, 12-HSA molecules spontaneously assemble into a three-dimensional network structure, which envelops the base oil and additives. This thermos-reversible transformation allows the materials to switch between an oily liquid and a semi-solid gel (**Fig. S2**). This unique property of the gel facilitates the prevention of environmental pollution caused by base oil creeping.

To investigative thermal properties of the supramolecular composite gels, the gel-sol transition temperature ($T_{gel-sol}$) and thermal stability of the 500 SN gel, UiO-67 gel, and UiO-67@PLMA gel were characterized using DSC and TGA. $T_{gel-sol}$ is an inherent property of amorphous systems, reflecting macroscopic transitions in molecular mobility. **Fig. 3a** shows DSC curves of different gels between 30 °C and 50 °C. All of the three gels display a single exothermic peak around 38 °C, corresponding to the gel-sol transition. Specifically, the $T_{gel-sol}$ value of the 500 SN gel and UiO-67 gel

were nearly identical, at 37.91 °C and 37.95 °C, the UiO-67@PLMA gel exhibited a slightly higher $T_{gel\text{-}sol}$ of 38.41 °C, suggesting that the presence of PLMA-modifed UiO-67 marginally increases the thermal stability of the composite gel structure. The thermal degradation behavior of the gels was evaluated via TGA (**Fig. 3b**). The 500 SN gel and UiO-67 gel began to decompose significantly at 230 °C and were fully decomposed at 393 °C. In contrast, the UiO-67@PLMA gel began decomposed by 413 °C. Thus, the enhancement in thermal stability is attributed to the improved interactions between the PLMA-modified MOF NPs and the gel matrix.

To further understand the gel-sol transition and its influence on mechanical performance, the rheological properties were measured as a function of temperature using a rotational rheometer. The viscoelastic behavior was assessed through the storage modulus (G') and loss modulus (G"), representing the elastic and viscous contribution, respectively. As shown in **Fig. 3c**, G' exceeded G" for all three samples (500 SN gel, UiO-67 gel, and UiO-67@PLMA gel) over 2.5 second, confirming that all materials exhibit viscoelastic solid-like behavior. The incorporation of UiO-67 increased both G' and G" moduli compared to the pristine 500 SN gel, indicating enhanced mechanical rigidity. Notably, the UiO-67@PLMA gel showed the highest values of G' and G" among the three, reflecting superior viscoelasticity and mechanical stability. This enhancement is attributed to the stronger hydrogen bonding between the PLMA brushes and the gel matrix, as opposed to the weaker physical entrapment of bare UiO-67 NPs [14].

Fig. 3d presents the shear viscosity of the gels as a function of shear rate. At low shear rates (< 100 s^{-1}), the viscosity of all gels dropped sharply, and the largest drop was attributed to UiO-67@PLMA gel with an initial viscosity of 38 Pa·s. At high shear rates (> 100 s^{-1}), the viscosities of all gels were stable and slowly declined to zero. Notably, UiO-67@PLMA gel owned the lowest viscosity compared to 500 SN gel and UiO-67 gel when the shear rate larger than 200 s^{-1}. This shear-thinning behaviour indicates the progressive breakdown of the 3D network of the gel under stress, which attributes to the disruption of hydrogen bonding and vdW interactions. Such rheological characteristics are

advantageous for lubricant applications, as they promote reduced resistance during mechanical operation.

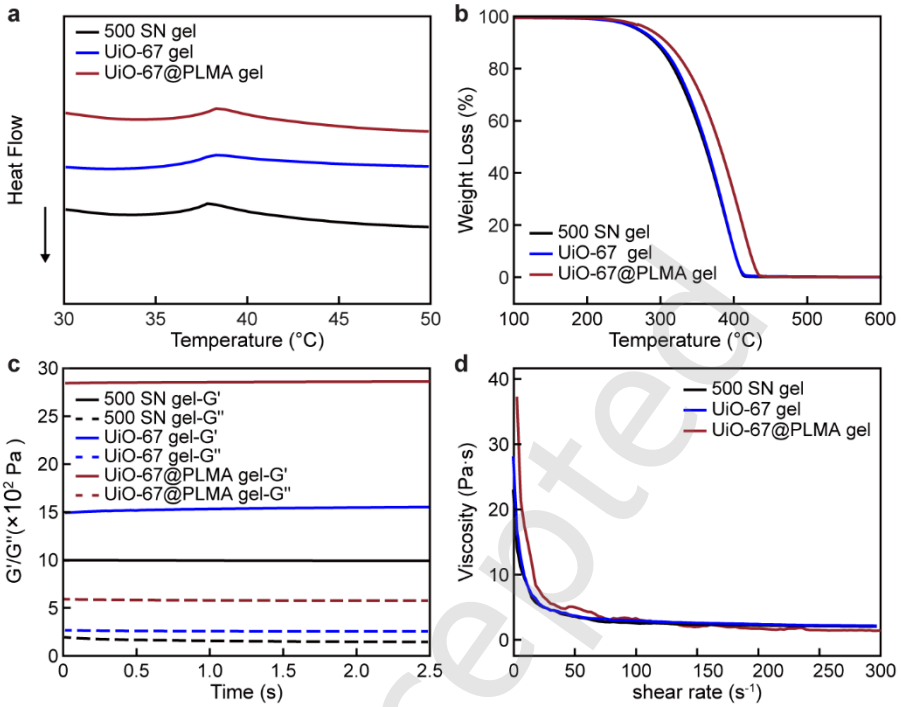

Fig. 3 Thermal and rheological properties of supramolecular composite gels with and without additives. (a) DSC curves measured between 30-50 °C in a N_2 atmosphere. (b) TGA thermograms. (c) G' and G″ as a function of time. (d) Shear viscosity of the gels as a function of shear rate.

3.5 Tribological properties of the UiO-67@PLMA as additives in 500 SN gel

Fig. 4 demonstrates the tribological performance of the UiO-67 NPs before and after PLMA brush grafting as additives in 500 SN gel by using SRV-V tribometer and 3D optical profilometer. The COF of pure 500 SN gel remained stable at 0.106 at the beginning of the test, which rapidly rose above 0.2 after 360 s, then gradually decreased and finally stabilized at 0.197 (**Fig. 4a**). For the gel with 0.4 wt.% UiO-67 NPs additive, the COF remained stable at 0.110 until 240 s, after which it increased and then stabilized at 0.196. In contrast, the addition of UiO-67@PLMA NPs significantly improved lubrication performance, maintaining a much lower and stable COF of 0.107 throughout the entire test.

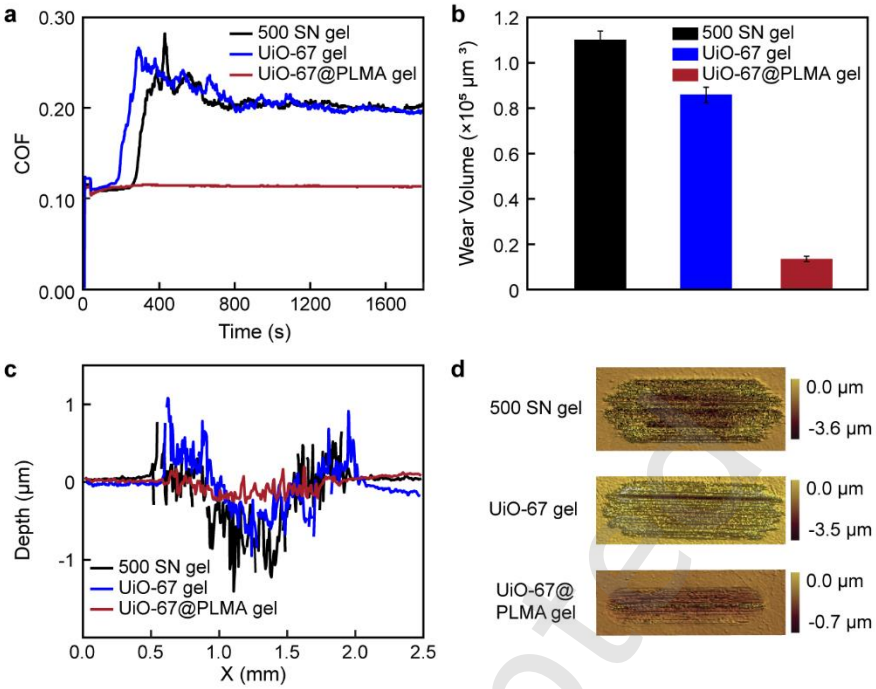

Fig. 4 Tribological properties of 0.4 wt.% UiO-67 NPs before and after PLMA grafting as additives in 500 SN gel. (a) COF curves, (b) wear volume, (c) cross-section profiles of wear scars, and (d) wear scar images of 500 SN gel, UiO-67 NPs gel, and UiO-67@PLMA NPs gel. (Load: 100 N; Temperature: 30 °C; Frequency: 25 Hz; Stroke: 1 mm)

Fig. 4b illustrates the wear volume on the steel disc after testing three gels under same conditions. Wear volume for the pure 500 SN gel was 1.12×10^5 μm^3. After adding 0.4 wt.% UiO-67 NPs in the 500 SN gel, the wear volume reduced to 0.82×10^5 μm^3. Remarkably, the wear volume for the UiO-67@PLMA gel decreased dramatically to 1.52×10^4 μm^3, representing an 86.42% reduction to compare with the 500 SN gel. Corresponding wear scar profiles and 3D images (**Figs. 4c-d**) revealed that the 500 SN gel left wide and rough wear scars with deep grooves, showing a wear depth of 1.12 μm. For the UiO-67 NPs additive, the depth decreased to 0.87 μm. Notably, the UiO-67@PLMA gel produced the shallowest and narrowest wear scars with wear depth of only 0.23 μm. These results demonstrate the excellent tribological performance offered by the UiO-67@PLMA additives in supramolecular composite gels.

To investigate the relationship between COF and addition concentration of UiO-67@PLMA NPs in supramolecular composite gels, tribological tests were performed with different concentrations ranging from 0.2 wt.% to 1.0 wt.% **(Fig. 5a)**. The COF for the pure 500 SN gel increased rapidly to 0.27 after 360 s, then decreased and stabilized at 0.198. By gradually increasing the concentration of UiO-67@PLMA (0.2 wt.%, 0.4 wt.%, and 0.6 wt.%), the COF remained consistently low and stable. At 1.0 wt.% concentration, however, the COF curve became unstable, with the lubricant showing delayed failure and a final COF of 0.187. As shown in **Fig. 5b**, wear volume decreased with increasing additive concentration up to 0.4 wt.%, reaching a minimum of 1.47×10^4 μm^3 with an 86.85% reduction to compare with pure 500 SN gel. Further increases in concentration resulted in higher wear volumes. In addition, cross-section profiles of wear scars further confirmed that 0.4 wt.% UiO-67@PLMA yielded the optimized concentration with the smallest and shallowest wear scars (**Figs. 5c-d**).

Fig. 6 presents a comprehensive study of the tribological performance of 500 SN gel, UiO-67 gel and UiO-67@PLMA supramolecular composite gel under various conditions of temperature, frequency, and load. For the effect of temperature, the COF of 500 SN gel remained stable at 0.112 up to 80 °C, after which it rose sharply to 0.181, then decreased and stabilized at 0.132 (**Fig. 6a**). The failure temperature was identified as 80 °C. In comparison, the UiO-67 gel displayed a slower COF rise up to 100 °C, peaking at 0.176 and stabilizing at 0.156. The UiO-67@PLMA gel exhibited superior thermal stability, with the COF increasing slowly to 0.138 up to 150 °C, then stabilizing at 0.134, indicating significantly improved temperature resistance. By increasing frequency from 10 N to 65 Hz, the 500 SN and UiO-67 gels failed at 15 Hz and 20 Hz, respectively (**Fig. 6b**). In contrast, the UiO-67@PLMA gel maintained stable lubrication throughout the entire frequency range, with a low COF of 0.105. **Fig. 6c** highlights the load-bearing capacity of the supramolecular composite gels. By adding UiO-67 NPs in the 500 SN gel, the load limit increased from 150 N to 200 N. Notably, with the UiO-67@PLMA NPs addition, the load limit further increased to 400 N. These results confirm that PLMA-

functionalized UiO-67 NPs significantly enhances the comprehensive tribological performance of 500 SN gels from 80 °C to 150 °C, 15 Hz to over 55 Hz, and 150 N to 400 N.

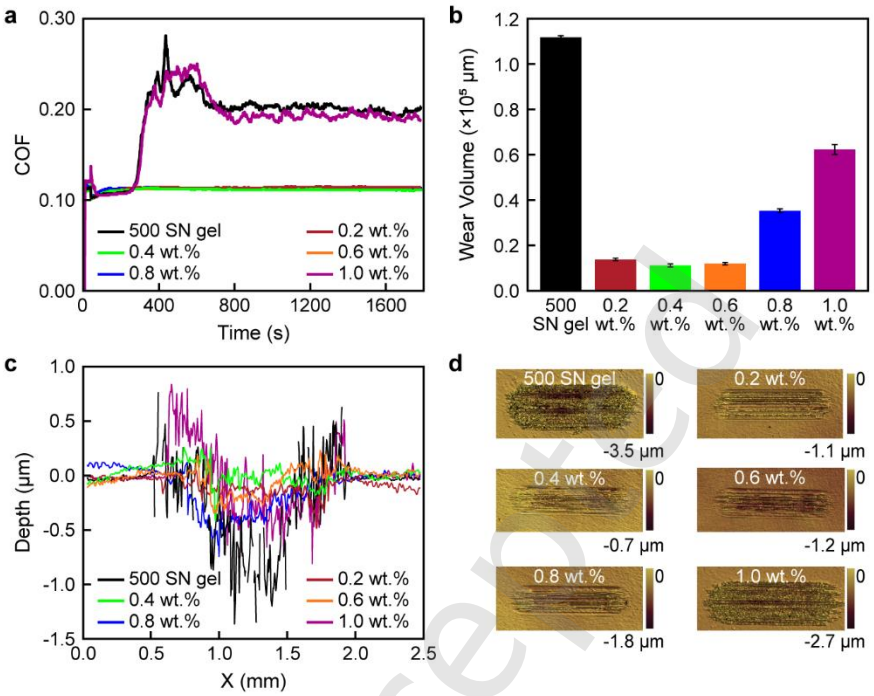

Fig. 5 Tribological properties of UiO-67@PLMA NPs as additive in 500 SN gel at varying concentrations. (a) COF curves, (b) wear volume, (c) cross-section profiles of wear scars, and (d) wear scar images for 500 SN gels containing UiO-67@PLMA NPs from 0.0 wt.% to 1.0 wt.%. (Load: 100 N; Temperature: 30 °C; Frequency: 25 Hz; Stroke: 1 mm)

In addition, we studied the yield of supramolecular composite gel by adding 12-HSA and UiO-67@PLMA NPs in PAO10 base oil as additives. The COF of the pure PAO10 gel initially stabilized at 0.108, then rose sharply to 0.292 due to abrasion, and gradually stabilized at 0.206 (**Fig. S3a**). With 0.4 wt.% UiO-67 additive, the COF increased rapidly to 0.24, then decreased to 0.198. When UiO-67@PLMA NPs was added, the COF stabilized at a much lower value of 0.105 throughout the test. As shown in **Fig. S3b**, the wear volume for PAO10 gel was 2.13×10^5 μm^3, which decreased to 1.47×10^5 μm^3 with UiO-67, and to 1.09×10^4 μm^3 with UiO-67@PLMA. **Figs. S3c-d** illustrate the corresponding wear scar morphologies of the supramolecular composite gels. Pure PAO10 gel caused wide, deep wear scars of 1.98 μm, while UiO-67 reduced the depth to 1.21 μm, and UiO-67@PLMA

further reduced it to only 0.15 μm. These findings indicate that 12-HAS combined with UiO-67@PLMA NPs significantly enhances the lubrication performance of PAO10 base oils as well.

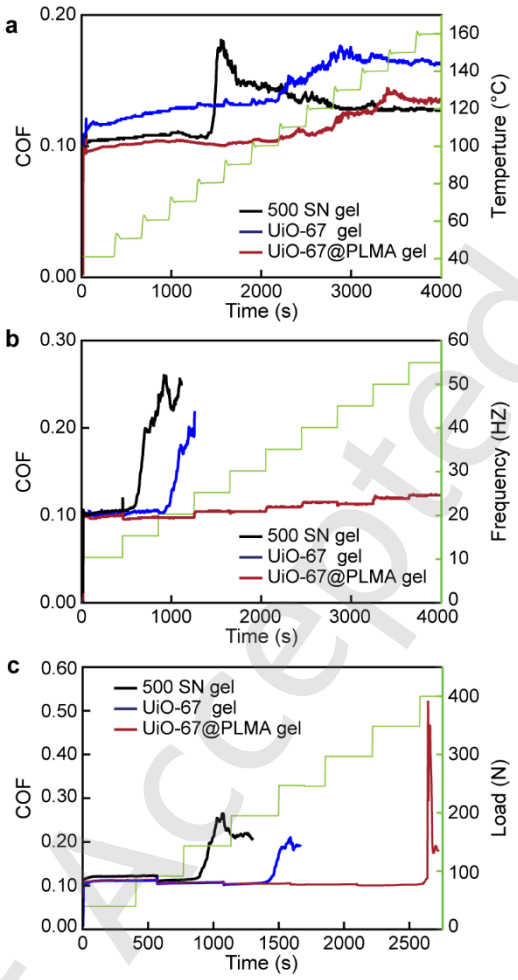

Fig. 6 Comprehensive tribological properties of UiO-67 NPs before and after PLMA grafting as additives in 500 SN gel. COF evolution under (a) temperature ramp (100 N, 25 Hz; Temperature increased from 40 °C to 160 °C at 10 °C/5 min), (b) frequency ramp (100 N, 30 °C; Frequency increased from 10 Hz to 65 Hz at 5 Hz/5 min), and (c) load ramp (30 °C, 25 Hz; Load increased from 50 N to 400 N at 50 N/5 min).

3.6 Lubricating mechanism analysis

For elucidating the anti-friction and anti-wear mechanisms of the UiO-67@PLMA additive of supramolecular composite gels, the micromorphology of the worn surfaces was examined by SEM. For the pure 500 SN gel, the SEM images revealed severe adhesive and fatigue wear, characterized by

spalling and extensive surface damage (**Figs. 7a-b**). With the addition of UiO-67 NPs in the gel, the wear surface exhibited numerous long-range grooves and irregularly distributed pits, indicative of abrasive and fatigue wear, along with minor adhesive wear (**Figs. 7c-d**). Nevertheless, when UiO-67@PLMA NPs were used as an additive, the worn surface appeared significantly smoother with much finer grooves and invisible damage (**Figs. 7e-f**). This improvement is attributed to the ball-bearing and polishing effects of the UiO-67@PLMA NPs, demonstrating their superior anti-wear performance.

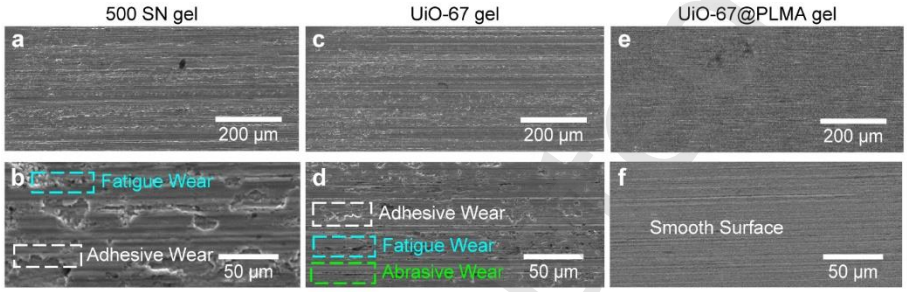

Fig. 7 SEM images of wear scars after tribological testing under constant condition (100 N; 30 °C; 25 Hz). (a-b) 500 SN gel. (c-d) UiO-67 NPs gel. (e-f) UiO-67@PLMA NPs gel.

To further elucidate the chemical composition on the wear surfaces, XPS was performed on the worn scar lubricated with UiO-67@PLMA gel. As shown in **Figs. 8a**, the full spectrum revealed characteristic Fe 2p peaks at 732.3, 727.6, 724.3, 719.8, and 711.2 eV, which can be assigned to Fe_2O_3 and FeOOH species (**Fig. 8b**). These findings align with O 1s peaks at 531.8 and 530.1 eV (**Fig. 8c**) [30]. Notably, no Zr 3d peaks were detected (**Fig. 8d**), suggesting that the Zr-based UiO-67 NPs did not directly contribute to the tribochemical layer, but rather facilitate indirect friction reduction. Overall, the XPS results confirm that a tribo-induced boundary layer composed of Fe_2O_3 and FeOOH forms on the wear surface, effectively lowering interfacial friction.

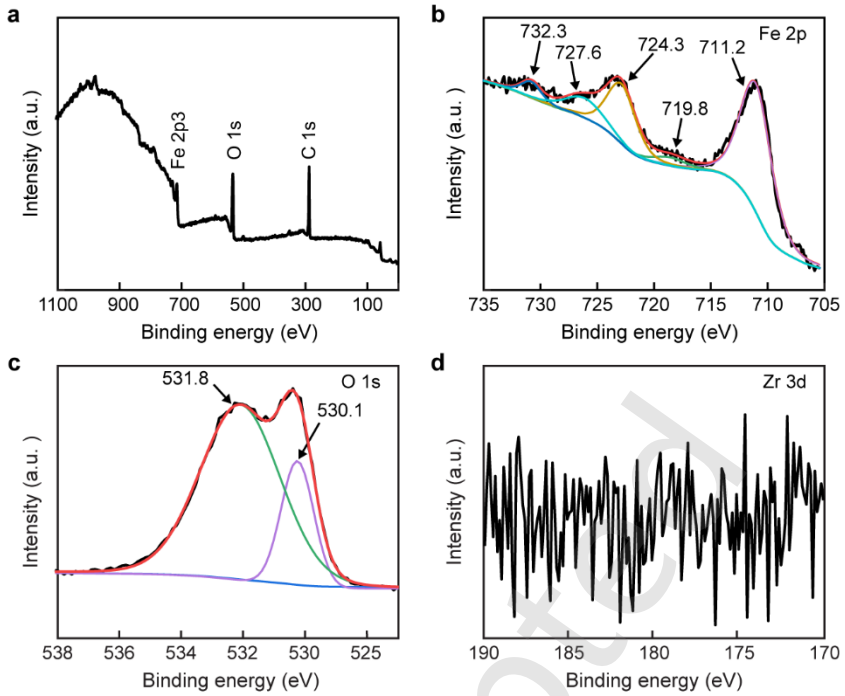

Fig. 8 XPS analysis of the worn steel surface after lubrication with UiO-67@PLMA NPs in 500 SN gel. (a) XPS full spectrum. XPS fine spectrums of (b) Fe 2p, (c) O 1s, and (d) Zr 3d.

Based on these observations, a lubrication mechanism for the UiO-67@PLMA-containing supramolecular composite gel is proposed (**Scheme 2**). During reciprocating sliding, shear causes the 3D supramolecular gel network, formed via hydrogen bonding and vdW interactions among 12-HSA molecules, to release both base oil and additives into the contact zone. The UiO-67@PLMA NPs, stabilized by polymer brushes, remain well-dispersed and act as nano ball-bearings, preventing direct surface contact. Meanwhile, a chemical reaction film (Fe_2O_3/FeOOH) and a physically absorbed layer of gel components synergistically contribute to enhanced friction reduction and wear protection.

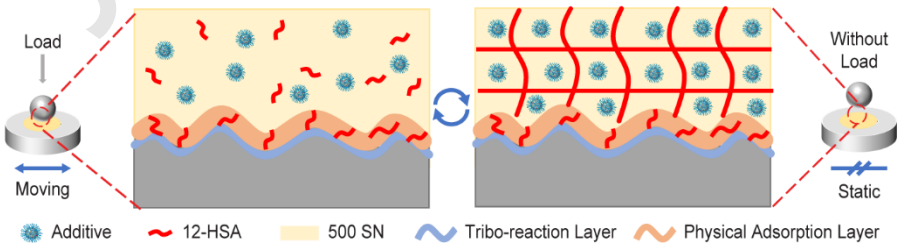

Scheme 2 Lubrication mechanism of UiO-67@PLMA as an additive in the supramolecular composite gel.

4 Conclusions

In summary, PLMA-grafted UiO-67 NPs have been demonstrated as highly effective lubricant additives in supramolecular composite gel, delivering outstanding anti-friction and anti-wear performance. The UiO-67 NPs were synthesized via a thermosolvent method and modified with PLMA brushes through SI-ATRP method, then dispersed in a 500 SN and PAO10 oil matrix and encapsulated within a 3D supramolecular network formed by 12-HAS. This structure suppressed based oil creep and prevented NPs sedimentation, which facilitates the application of nanoadditives in lubrication gel. Tribological tests revealed that incorporating 0.4 wt.% UiO-67@PLMA reduced the COF by 45.68% and wear volume by over 86.85%, while significantly enhancing the load-bearing capacity from 50 N to 400 N, and maintaining stable performance under variable temperature and frequency. These lubrication enhancements are attributed to the synergistic effect of: (1) the ball-bearing and polishing actions of UiO-67@PLMA NPs and the base oil released during reciprocating motion, (2) the formation of a tribochemical protective film on the steel substrate, and (3) the adsorption of 12-HSA and oil components on the friction interface, forming a stable physical lubrication film.

Acknowledgements

This work was supported by the National Natural Science Foundations of China (52475216) and the State Key Laboratory of Solid Lubrication (LSL-2401). We would like to thank the Analytical & Testing Center of Northwestern Polytechnical University and Shaanxi Materials Analysis and Research Center.

Declaration of competing interest

The authors have no competing interests to declare that are relevant to the content of this article.

Electronic Supplementary Material

Supplementary material is available in the online version of this article at….

References

[1] Bianco S, Hasan M, Ahmad A, Richards S-J, Dietrich B, Wallace M, Tang Q, Smith AJ, Gibson MI and Adams DJ, Mechanical release of homogenous proteins from supramolecular gels. *Nature* **631**(8021): 544-548 (2024)

[2] Bianco S, Hallam Stewart F, Panja S, Zyar A, Bowley E, Bek M, Kádár R, Terry A, Appio R, Plivelic TS, Maguire M, Poptani H, Marcello M, Sonani RR, Egelman EH and Adams DJ, Forging out-of-equilibrium supramolecular gels. *Nat. Synth.* **3**(12): 1481-1489 (2024)

[3] Zhang J, Jiang D, Wang D, Yu Q, Bai Y, Cai M, Weng L, Zhou F and Liu W, MoS2 lubricating film meets supramolecular gel: A novel composite lubricating system for space applications. *ACS Appl. Mater. Interfaces* **13**(48): 58036-58047 (2021)

[4] Wang T, Wang Y, Wang X, He B, Liu S, Ye Q, Zhou F and Liu W, Fabrication of ionic supramolecular oleogel lubricants enhanced with liquid metal nanodroplets for superior tribological performance. *ACS Nano* **18**(49): 33468–33478 (2024)

[5] Takahashi K, Shitara Y, Kaimai T, Kanno A and Mori S, Lubricating properties of TR Gel-lube—Influence of chemical structure and content of gel agent. *Tribol. Int.* **43**(9): 1577-1583 (2010)

[6] Chakravarthy RD, Sahroni I, Wang C-W, Mohammed M and Lin H-C, Temperature-induced nanostructure transition for supramolecular gelation in water. *ACS Nano* **17**(12): 11805-11816 (2023)

[7] Ke H, Yang LP, Xie M, Chen Z, Yao H and Jiang W, Shear-induced assembly of a transient yet highly stretchable hydrogel based on pseudopolyrotaxanes. *Nat Chem* **11**(5): 470-477 (2019)

[8] Chen Q, Chen K, Zhang X, Feng H, Feng C, Li X and Zhang D, Recent progress of hydrogel-based biomimetic articular cartilage in mechanical and lubricated enhancement. *Friction*: (2025)

[9] Minakuchi N, Hoe K, Yamaki D, Ten-no S, Nakashima K, Goto M, Mizuhata M and Maruyama T, Versatile supramolecular gelators that can harden water, organic solvents and ionic liquids. *Langmuir* **28**(25): 9259-9266 (2012)

[10] Yu Q, Huang G, Cai M, Zhou F and Liu W, In situ zwitterionic supramolecular gel lubricants for significantly improved tribological properties. *Tribol. Int.* **95**: 55-65 (2016)

[11] Bai Y, Hu X, Zhang M, Yu Q, Liang Y, Wu Y, Cai M, Zhou F and Liu W, Improving compatibility and tribological performance via supramolecular gelation of MoS2 nanoparticles in Perfluoropolyether lubricants. *Friction*: (2025)

[12] Bai Y, Yu Q, Zhang J, Cai M, Liang Y, Zhou F and Liu W, Soft-nanocomposite lubricants of supramolecular gel with carbon nanotubes. *Journal of Materials Chemistry A* **7**(13): 7654-7663 (2019)

[13] Zhang R, Liu X, Guo Z, Cai M and Shi L, Effective sugar-derived organic gelator for three different types of lubricant oils to improve tribological performance. *Friction* **8**(6): 1025-1038 (2020)

[14] Guo J, Zeng C, Wu P, Liu G, Zhou F and Liu W, Surface-functionalized Ti3C2Tx MXene as a kind of efficient lubricating additive for supramolecular gel. *ACS Appl. Mater. Interfaces*: (2022)

[15] Lu W, Wei Z, Gu ZY, Liu TF, Park J, Park J, Tian J, Zhang M, Zhang Q, Gentle T, 3rd, Bosch M and Zhou HC, Tuning the structure and function of metal-organic frameworks via linker design. *Chem. Soc. Rev.* **43**(16): 5561-93 (2014)

[16] Yang X, Wang Y, Cao W, Zheng J, Liu C, Fan B and Qi X, Flexible metal–organic frameworks based self-lubricating composite. *Friction* **12**(8): 1816-1827 (2024)

[17] Liu J, Luo H, Li Z, Peng Y, Zhang J, Khaniyev B, Mukhametkarimov Y, Ibraimov M and Xu Y, Designing hybrid plasmonic superlattices with spatially confined responsive heterostructural units. *Nano Lett.* **25**(2): 754–761 (2025)

[18] Furukawa H, Cordova KE, O'Keeffe M and Yaghi OM, The chemistry and applications of metal-organic frameworks. *Science* **341**(6149): 1230444 (2013)

[19] LUO Haowen, Li Fanfan, WU Wei, LI Xuguang, QIAN Yong, ZHANG Mengchen and LIU Jianxi, Preparation of DDP-functionalized UiO-66 nanoparticles and tribological properties as lubricating oil additives. *TRIBOLOGY* **44**(8): 1064−1073 (2024)

[20] Wang F-F, Liu Z and Cheng Z-L, High performance of MOF-structured lubricating material with nano- and micro-sized morphologies. *Mater. Lett.* **248**: 222-226 (2019)

[21] Wang Y-H, Shi Q, Xu H and Dong J-X, The synthesis and tribological properties of small- and large-sized crystals of zeolitic imidazolate framework-71. *RSC Advances* **6**(22): 18052-18059 (2016)

[22] Sun D, Wong LW, Wong HY, Lai KH, Ye L, Xv X, Ly TH, Deng Q and Zhao J, Direct visualization of atomic structure in multivariate metal-organic frameworks (MOFs) for guiding electrocatalysts design. *Angew. Chem. Int. Ed.* **62**(4): e202216008 (2023)

[23] Luo H, Zhang Y, Lv Z, Luo S, Ou Y, Xue H, Wang G-E, Xu G and Liu J, Engineering surface functional groups of 2D organic metal chalcogenides to regulate lubrication performance across scales. *Tribol. Int.* **204**: 110420 (2024)

[24] Wu W, Liu J, Li Z, Zhao X, Liu G, Liu S, Ma S, Li W and Liu W, Surface-functionalized nanoMOFs in oil for friction and wear reduction and antioxidation. *Chem. Eng. J.* **410**: 128306 (2021)

[25] Liu J, Luo H, Qian Y, Li F, Wu W, Yi X, Shi J, Tian Y and Zhang S, DDP-functionalized UiO-67 nanoparticles as lubricating oil additives for friction and wear reduction. *Tribol. Int.* **186**: 108627 (2023)

[26] Liu J, Qian Y, Li D, Wu W, Zhang M, Yan J, Li B and Zhou F, Oil-soluble polymer brushes-functionalized nanoMOFs for highly efficient friction and wear reduction. *Friction* **12**: 1499-1511 (2024)

[27] Du M, Cao Y, Luo X, Yang W, Lin W, Wang Y, Tang W and Li Z, Shapeable sodium alginate aerogel beads incorporated with L-cysteine-modified defective UiO-67 for heavy metal ions removal. *Chem. Eng. J.* **475**: 146289 (2023)

[28] He S, Wang H, Zhang C, Zhang S, Yu Y, Lee Y and Li T, A generalizable method for the construction of MOF@polymer functional composites through surface-initiated atom transfer radical polymerization. *Chem Sci* **10**(6): 1816-1822 (2019)

[29] Wu M, Wu M, Pan M, Jiang F, Hui B and Zhou L, Synthesization and characterization of lignin-graft-Poly (Lauryl Methacrylate) via ARGET ATRP. *Int. J. Biol. Macromol.* **207**: 522-530 (2022)

[30] Guo J, Wu P, Zeng C, Wu W, Zhao X, Liu G, Zhou F and Liu W, Fluoropolymer grafted Ti3C2Tx MXene as an efficient lubricant additive for fluorine-containing lubricating oil. *Tribol. Int.* **170**: 107500 (2022)

Author biography

Yong Qian. He received his Bachelor degree and Master degree in Materials Science and Engineering in 2021 from University of South China and in the Center of Advanced Lubrication and Sealing Materials in 2024 from Northwestern Polytechnical University. His research interests include MOFs-based nanocomposite materials and their lubrication properties.

Haowen Luo. He earned his Master degree in Materials Science in 2025 following a Bachelor of Materials Forming and Control Engineering in School of Materials Science and Engineering, Northwestern Polytechnical University. He currently is a Ph.D. student at Department of Chemistry,

City University of Hong Kong. His research interests focus on the nanotribology of 2D materials and their modulation strategies.

Jianxi Liu. He is a professor in the School of Materials Science and Engineering at Northwestern Polytechnical University. Before taking this position, he worked as a postdoctoral researcher at Northwestern University from 2016 to 2018. He received his Ph.D. degree from Karlsruhe Institute of Technology in 2015. His current research interests focus on smart lubrication, multifunctional coatings, nanotribology, and optical sensing.